




## Article

# Morphology of Phagophore Precursors by Correlative Light-Electron Microscopy

Sigurdur Runar Gudmundsson<sup>1,2</sup>, Katri A. Kallio<sup>1</sup>, Helena Vihinen<sup>3</sup> , Eija Jokitalo<sup>3</sup> , Nicholas Ktistakis<sup>4</sup> and Eeva-Liisa Eskelinen<sup>5,\*</sup> 

<sup>1</sup> Molecular and Integrative Biosciences, University of Helsinki, 00790 Helsinki, Finland

<sup>2</sup> Biomedical Center, School of Health Sciences, University of Iceland, 101 Reykjavik, Iceland

<sup>3</sup> Institute of Biotechnology, University of Helsinki, 00790 Helsinki, Finland

<sup>4</sup> Babraham Institute, Cambridge CB22 3AT, UK

<sup>5</sup> Institute of Biomedicine, University of Turku, 20520 Turku, Finland

\* Correspondence: eeva-liisa.eskelinen@utu.fi; Tel.: +358-505115631

**Abstract:** Autophagosome biogenesis occurs in the transient subdomains of the endoplasmic reticulum that are called omegasomes, which, in fluorescence microscopy, appear as small puncta, which then grow in diameter and finally shrink and disappear once the autophagosome is complete. Autophagosomes are formed by phagophores, which are membrane cisterns that elongate and close to form the double membrane that limits autophagosomes. Earlier electron-microscopy studies showed that, during elongation, phagophores are lined by the endoplasmic reticulum on both sides. However, the morphology of the very early phagophore precursors has not been studied at the electron-microscopy level. We used live-cell imaging of cells expressing markers of phagophore biogenesis combined with correlative light-electron microscopy, as well as electron tomography of ATG2A/B-double-deficient cells, to reveal the high-resolution morphology of phagophore precursors in three dimensions. We showed that phagophores are closed or nearly closed into autophagosomes already at the stage when the omegasome diameter is still large. We further observed that phagophore precursors emerge next to the endoplasmic reticulum as bud-like highly curved membrane cisterns with a small opening to the cytosol. The phagophore precursors then open to form more flat cisterns that elongate and curve to form the classically described crescent-shaped phagophores.

**Keywords:** autophagy; phagophore; isolation membrane; omegasome; ATG13; DFCP1; ATG2; correlative light-electron microscopy



check for

**Citation:** Gudmundsson, S.R.; Kallio, K.A.; Vihinen, H.; Jokitalo, E.; Ktistakis, N.; Eskelinen, E.-L. Morphology of Phagophore Precursors by Correlative Light-Electron Microscopy. *Cells* **2022**, *11*, 3080. <https://doi.org/10.3390/cells11193080>

Academic Editor: Nikolai Engedal

Received: 18 July 2022

Accepted: 23 September 2022

Published: 30 September 2022

**Publisher's Note:** MDPI stays neutral with regard to jurisdictional claims in published maps and institutional affiliations.



**Copyright:** © 2022 by the authors. Licensee MDPI, Basel, Switzerland. This article is an open access article distributed under the terms and conditions of the Creative Commons Attribution (CC BY) license (<https://creativecommons.org/licenses/by/4.0/>).

membranes) nucleate and elongate inside omegasomes. When the phagophore reaches maturity, it fuses to form a double-membraned autophagosome, and the DFCP1-positive omegasome shrinks and disappears. Autophagosomes subsequently fuse with endosomes to form amphisomes [6], where acidification starts. Amphisomes eventually fuse with lysosomes to form autolysosomes [7], where the bulk of the cargo degradation occurs, and the metabolites are then recycled through the autolysosomal membrane back to the cytoplasm.

Phagophores have also been demonstrated to nucleate from recycling endosomes and subsequently make membrane contact sites (MCSs) with other organelles, mainly the ER, in order to elongate [8–10]. Multiple other organelles have also been reported as membrane

## 2.2. CLEM with Serial Block-Face-Imaging Scanning Electron Microscopy (SBEM)

After live-cell imaging, the cells were fixed again in 2.5% glutaraldehyde (Sigma, G5882) in 0.1 M sodium cacodylate buffer (pH 7.4), supplemented with 2 mM  $\text{CaCl}_2$  and postfixed using double osmication prior to uranyl acetate en bloc staining and lead aspartate treatment, as described previously [26]. The method was modified from [27]. Finally, the cells were dehydrated and embedded in resin (Fluka, Durcupan ACM) between

cells were fixed in 4% paraformaldehyde in 0.2 M HEPES buffer (pH 7.4) for 10 min, permeabilized in 0.1% Triton X-100 in phosphate-buffered saline (PBS) (pH 7.4) for 10 min and blocked with 1% bovine serum albumin at room temperature for 3 h. The cells were labeled with mouse monoclonal anti-human transferrin receptor (TfR) (Invitrogen 136,800) at 1:200 dilution, or anti-ATG2B (Thermo Fisher 25155-1-AP) at 1:200 dilution, in 0.1% bovine serum albumin in PBS at +4 °C overnight. After washing in PBS, the cells were labeled with Alexa

**Figure 1.** CLEM of an omegasome and a nascent phagophore/autophagosome. **(A)** HEK293 cells expressing GFP-tagged DFCP1 were time-lapse imaged to trace omegasomes. After fixation, the same cell and omegasome were imaged with electron tomography. **(B)** One slice of the tomogram overlaid with the DFCP1 fluorescence. **(C)** The phagophore, ER, lysosomes and mitochondria were traced to create a 3D model, using the color code shown in the top right corner of the figure. Panel **(C)** shows one tomography slice overlaid with part of the 3D model. **(D)** The 3D model shows the relationships of the phagophore, ER, mitochondria and lysosomes with each other. **(E)** The DFCP1 fluorescence from live-cell imaging overlaid with the 3D model. Note that the DFCP1 localization overlaps the ER in the 3D model. **(F–H)** Slices through the tomogram. Panels **(F–H')** show the boxed areas at higher magnification. **(F,F')** The phagophore/autophagosome (green arrows) has MCSs (red arrows in **(F')**) with the ER (yellow arrows) inside and outside of the phagophore. **(G,G')** The phagophore/autophagosome (green arrows) has MCSs with a lysosome (Ly). **(H,H')** The phagophore/autophagosome (green arrows) also has an MCS (white arrow in **(H')**) with a mitochondrion (mi). In panels **(D,E)**, ER, mitochondria and lysosomes are shown as volume rendered according to their grey-level values. See also Supplementary Figure S1.



To summarize, the ATG2A/B-deficient cells are able to form phagophore precursors/small autophagosomes of approximately 200 nm in diameter in the regions rich in cup-shaped 50–60 nm vesicles.

### *3.3. ATG13-Positive Phagophore Precursor Localizes in Proximity to ATG2 but Not TfR*

ATG13 is a subunit of the ULK1 complex that initiates phagophore biogenesis by translocating to the ER [4,36]. In order to visualize the earliest steps of phagophore biogenesis with correlative light-electron microscopy (CLEM), we used HEK293 cells expressing GFP-ATG13, which were used earlier to demonstrate that GFP-ATG13 puncta mark sites of phagophore biogenesis [4]. In addition to the ER, recycling endosomes have also been implicated in the nucleation or biogenesis of phagophores [8–10,37,38]. As stated above, ATG2 localizes at the ER–phagophore MCSs, where it transfers lipids from the ER to the expanding phagophore [







Figure 4.

Figures 3 and 4. Tomography of this punctum revealed an open slightly bent phagophore (Figure 5E,E',H) that showed MCSs with the ER at the edge of the cistern and with the convex surface of the curved cistern (Figure 5E,E',F,F'). A bundle of filaments, likely actin filaments, were located next to the phagophore (Figure 5F,F',I,J).

**Figure 5.** CLEM of a phagophore. (A) HEK293 cells expressing GFP-tagged ATG13 were time-lapse imaged to trace ATG13 puncta. The cells were fixed 4 min 45 s after the appearance of the ATG13 punctum. After fixation, the same cell and punctum were imaged with electron tomography. (B) One slice of the tomogram overlaid with the ATG13 fluorescence. (C–F) Tomography slices showing the phagophore (green arrows), ER (yellow arrows), vesicles (purple arrows) and a bundle of putative actin filaments (pink arrows). The white arrow in panel (C) indicates an MCS between a mitochondrion (mi) and ER close to the phagophore. (G) Organelles in the tomogram were traced with different colors, as indicated by the overlay, as well as the bottom right panel of the figure. Panels (C',E',F') show enlarged details from panels (C,E,F), respectively. The red arrows in panels (E',F') indicate MCSs between the phagophore and ER. (H

it can form additional MCSs with the ER and other organelles, which might correspond to multiple lipid-transfer sites to the elongating phagophore.

#### **4. Discussion**

In this study, we visualized phagophore biogenesis in relation to the ER subdomain,

---

observed 30–60 nm vesicles, many of them cup-shaped, next to the phagophore precursors

*Cells*

28. Belevich, I.; Joensuu, M.; Kumar, D.; Vihinen, H.; Jokitalo, E. Microscopy Image Browser: A Platform for Segmentation and Analysis of Multidimensional Datasets. *PLoS Biol.* **2016**, *14*, e1002340. [[CrossRef](#)]
29. Fedorov, A.; Beichel, R.; Kalpathy-Cramer, J.; Finet, J.; Fillion-Robin, J.C.; Pujol, S.; Bauer, C.; Jennings, D.; Fennessy, F.; Sonka, M.; et al. 3D Slicer as an image computing platform for the Quantitative Imaging Network. *Magn. Reson. Imaging* **2012**, *30*, 1323–1341. [[CrossRef](#)]
30. Mastronarde, D.N. Automated electron microscope tomography using robust prediction of specimen movements. *J. Struct. Biol.* **2005**, *152*, 36–51. [[CrossRef](#)]
31. Kremer, J.R.; Mastronarde, D.N.; McIntosh, J.R. Computer visualization of three-dimensional image data using IMOD. *J. Struct. Biol.* **1996**, *116*, 71–76. [[CrossRef](#)]
32. Cardona, A.; Saalfeld, S.; Schindelin, J.; Arganda-Carreras, I.; Preibisch, S.; Longair, M.; Tomancak, P.; Hartenstein, V.; Douglas,